

Excessive Exoergicity Reduces Singlet Exciton Fission Efficiency of Heteroacenes in Solutions

You-Dan Zhang,[†] Yishi Wu,[‡] Yanqing Xu,[§] Qiang Wang,[†] Ke Liu,[†] Jian-Wei Chen,[‡] Jing-Jing Cao,[†] Chunfeng Zhang,[§] Hongbing Fu,^{*,‡} and Hao-Li Zhang^{*,†}

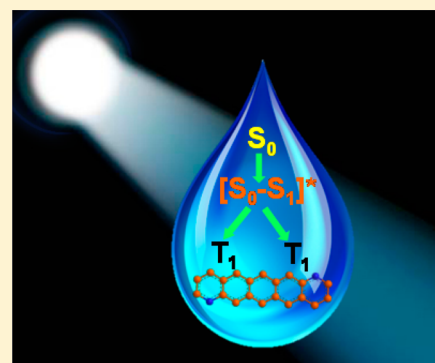
[†]State Key Laboratory of Applied Organic Chemistry (SKLAOC), Key Laboratory of Special Function Materials and Structure Design (MOE), College of Chemistry and Chemical Engineering, Lanzhou University, Lanzhou 730000, P. R. China

[‡]Beijing National Laboratory for Molecules Science (BNLMS), State Key Laboratory for Structural Chemistry of Unstable and Stable Species, and Key Laboratory of Photochemistry, Institute of Chemistry, Chinese Academy of Sciences, Beijing 100190, P. R. China

[§]National Laboratory of Solid State Microstructures, School of Physics, and Collaborative Innovation Center of Advanced Microstructures, Nanjing University, Nanjing 210093, China

S Supporting Information

ABSTRACT: The energy difference between a singlet exciton and twice of a triplet exciton, ΔE_{SF} , provides the thermodynamic driving force for singlet exciton fission (SF). This work reports a systematic investigation on the effect of ΔE_{SF} on SF efficiency of five heteroacenes in their solutions. The low-temperature, near-infrared phosphorescence spectra gave the energy levels of the triplet excitons, allowing us to identify the values of ΔE_{SF} , which are -0.58 , -0.34 , -0.31 , -0.32 , and -0.34 eV for the thiophene, benzene, pyridine, and two tetrafluorobenzene terminated molecules, respectively. Corresponding SF efficiencies of the five heteroacenes in 0.02 M solutions were determined via femtosecond transient absorption spectroscopy to be 117%, 124%, 140%, 132%, and 135%, respectively. This result reveals that higher ΔE_{SF} is not, as commonly expected, always beneficial for higher SF efficiency in solution phase. On the contrary, excessive exoergicity results in reduction of SF efficiency in the heteroacenes due to the promotion of other competitive exciton relaxation pathways. Therefore, it is important to optimize thermodynamic driving force when designing organic materials for high SF efficiency.



1. INTRODUCTION

Singlet exciton fission (SF)¹ is a process in which a photogenerated higher energy singlet exciton is converted into two triplet excitons of lower energy with a nearby ground-state molecule. SF is drawing increasing attention recently mainly due to its potential capability to break the semiempirical Shockley-Queisser (SQ) limit in single-junction solar cells.^{2–4} The realizations of SF in solar cell devices have been reported by several groups.^{4–6} Baldo et al. demonstrated that external quantum efficiency above 100% was achieved in a SF-based organic solar cell, suggesting promising applications of SF materials in photovoltaic devices.⁵

One of the thorniest problems of SF is that the number of molecules exhibiting SF is still limited.^{7–12} Up to now, the most studied SF system has been acene family,^{13–24} such as pentacene. Recently, a few new families of small molecules and polymers have been reported to show high efficient SF.^{7,11,12,25,26} Design of novel organic molecules with high SF efficiency requires fundamental understanding of the structure–property correlation in different organic molecules. The most basic question needing answer is how to optimize molecular structures for high SF efficiency. From theoretical perspective, two parameters mainly govern the SF process,

which are the thermodynamic driving force (ΔE_{SF}) and the electronic coupling.^{7,27–30} The ΔE_{SF} is defined as $2E(T_1) - E(S_1)$,^{16,31,32} in which $E(T_1)$ is the energy level of triplet exciton, while $E(S_1)$ is the energy level of singlet exciton. Meanwhile, the electronic coupling between a singlet exciton and a nearby ground-state molecule is believed to govern the energy transfer rate during the exciton fission. Yaffe et al. demonstrated that pentacene is the most efficient in acene family due to optimal ΔE_{SF} in solid films.¹⁶ Our recent work suggested that strong electronic coupling promotes SF efficiency in crystalline heteropentacene.²⁸

A majority of the present researches on SF were conducted in solid states, in which the above two effects take place simultaneously, making identifying their individual role on SF efficiency difficult.⁸ The preference of studying SF in crystalline state is mainly due to consideration that SF process requires strong exciton coupling,^{29,33–35} while crystalline structures give the closest molecular packing. However, Bradforth et al. have reported the observation of SF in an amorphous solid of a

Received: November 22, 2015

Revised: April 13, 2016

Published: May 11, 2016

tetracene derivative, suggesting that long-range order is not required for SF.³⁶ New opportunity comes from the report by Friend et al., who found that SF could occur efficiently in solutions with triplet yield reaching close to 200%.²³ Highly efficient SF processes in solutions were also reported by a few other groups, including covalently attached dimers^{14,15,18,20,24} and monomers, like pentacene²³ and tetracene²¹ derivatives. The dimers and monomers behave quite differently, as SF in covalently attached dimers is geometrically constrained, while the monomers require high concentrations in order for dimer pairs to form sufficiently quickly for fission to proceed. The realization of SF in solutions opens more opportunities for not only further understanding of the mechanism of the SF process but also the applications of triplet exciton, as the long lifetimes of triplet excitons generated in solutions by SF are highly desirable for applications like photocatalysis. Recently, we have demonstrated that SF can induce giant optical limiting responses in pentacene derivatives associated with strong triplet absorption.^{37,38}

Because very few investigations on the SF in solution have been conducted, the understanding of many basic issues is still very limited. The main purpose of this study is to understand the role of ΔE_{SF} on SF process of monomers taking place in solutions. Previously, there have been only two studies trying to probe the role of ΔE_{SF} : one was performed using three solid acenes with distinctly different molecular structures and packing,¹⁶ while the other one was conducted using theoretical calculations.³⁹ Whether the conclusion obtained from solid is also applicable to acenes in solution remain unknown. Moreover, studies on molecular solutions may overcome the interplay problem between ΔE_{SF} and molecular packing that is difficult to avoid in solid. In solutions, for compounds with similar structures, the packing models in solutions resemble with each other. Thus, it is reasonable to assume that the contributions of electronic couplings of these five heteroacenes to SF are similar to each other, so that ΔE_{SF} plays the dominate role. Therefore, acenes in solution phase shall provide an ideal model system for understanding the role of ΔE_{SF} .

Herein, we conducted an investigation on SF in solutions of five heteroacenes with similar five-ring fused structures as shown in Figure 1. The energy levels and molecular packing of these molecules in solid state have been thoroughly studied in our previous research,^{40–42} which suggested that they exhibit similar 2-D stacking in their crystals. When the two terminal rings are changed to thiophene, benzene, pyridine, pyrazine, and tetrafluorobenzene, the energy levels of singlet exciton ($E(S_1)$) and triplet excitons ($E(T_1)$) can be tuned effectively, which helps to unveil the effects of exciton energy level on the SF efficiency.

2. RESULTS AND DISCUSSION

The mechanism of SF in solutions is schematically illustrated in Figure 1b,²³ which process is briefly described below. First, one molecule in the ground state absorbs a photon above a certain energy to form a singlet excited state, S_1 . Then, the singlet excited state interacts with a nearby ground-state molecule to form a stable species, $[S_0-S_1]^*$, excimer, of which the energy is more than twice that of triplet state. The intermediate state in concentrated solutions has been identified and optically observed by Stern group.²¹ The excimer then faces two competitive ways to channel out: it can either emit directly (Figure S4) or decay rapidly into two separated triplets, which may return to the ground state by emitting phosphorescence.

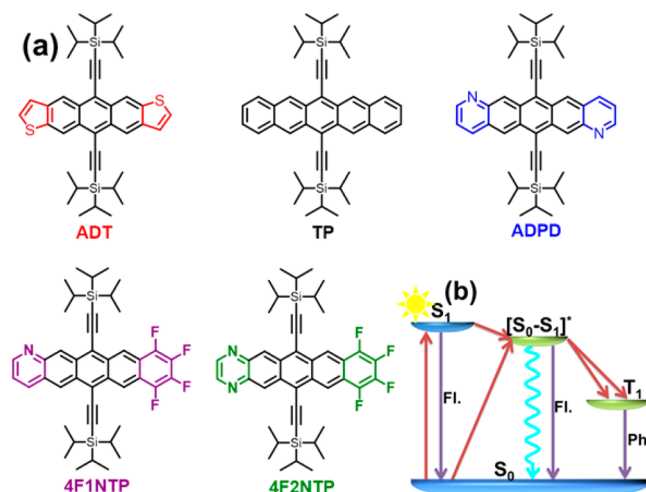


Figure 1. (a) Molecular structures of ADT, TP, ADPD, 4F1NTP, and 4F2NTP. (b) Illustration to the mechanism of SF in solutions: one singlet-excited molecule and one nearby ground-state molecule form an excimer $[S_0-S_1]^*$; then, the excimer intermediate decays to two triplets. The cyan curve is the nonradiative decay of the excimer.

One common and efficient strategy to adjust the energy levels and the triplet yields of acene derivatives is by introducing heterocycles and fluorine atoms into the acene framework.³⁹ In our previous studies, we have designed a series of S and N containing and fluorinated heteroacenes and systematically studied how their molecular energy levels correlated to their electronic properties.^{40–43} Herein, we selected one pentacene derivative, one S containing pentacene analogue, and three N-heteropentacenes to explore the effect of energy levels on the SF process. The five molecules are bis(triisopropylsilylethynyl)anthradithiophene (ADT), bis(triisopropylsilylethynyl)pentacene (TP), 6,13-bis(triisopropylsilylethynyl)anthradipyridine (ADPD), 8,9,10,11-tetrafluoro-6,13-bis(triisopropylsilylethynyl)-1-azapentacene (4F1NTP), and 8,9,10,11-tetrafluoro-6,13-bis(triisopropylsilylethynyl)-1,4-diazapentacene (4F2NTP), whose structures are shown in Figure 1a.

The positions of the frontier molecular orbitals, including the highest occupied molecular orbitals (HOMOs) and the lowest unoccupied molecular orbitals (LUMOs), of the five molecules are illustrated in Figure 2d, which were obtained from cyclic voltammetry methods (Figure S2). The TP molecule has LUMO and HOMO levels at -3.08 and -5.18 eV, respectively. When the two benzene rings are replaced by thiophene rings, the ADT molecule shows a rise of LUMO to -2.98 eV and a drop of HOMO to -5.25 eV. In contrast, replacing both the two terminal benzene rings by pyridine rings lowers the frontier orbital levels, and the ADPD has HOMO and LUMO at -5.42 and -3.40 eV, respectively. The energy gaps of TP and ADPD are nearly the same, about 1.85 eV, smaller than the energy gap of ADT of 2.20 eV. When the benzene rings are replaced by electron-drawing tetrafluorobenzene or pyrazine, the HOMO and LUMO energy levels are decreased further. For 4F1NTP and 4F2NTP, the HOMOs are at -5.49 and -5.51 eV, and the LUMOs are at -3.46 and -3.61 eV, respectively. The energy bandgaps of 4F1NTP and 4F2NTP are 1.87 and 1.83 eV, respectively.

Figure 2a shows the steady-state UV–visible absorption spectra of ADT, TP, ADPD, 4F1NTP and 4F2NTP in toluene solutions. The TP, ADPD, 4F1NTP and 4F2NTP molecules

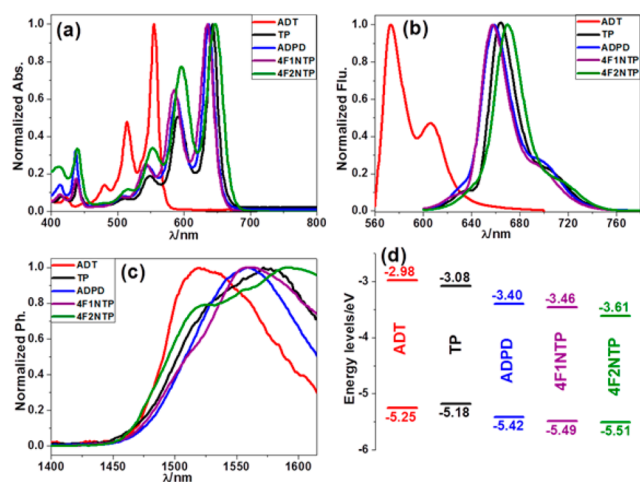


Figure 2. (a) UV–visible absorption and (b) fluorescence emission spectra of ADT, TP, ADPD, 4F1NTP, and 4F2NTP in dilute toluene solutions, and (c) phosphorescence emission spectra of ADT, TP, ADPD, 4F1NTP, and 4F2NTP in toluene solutions with optical density less than 0.1 at the excitation wavelength. (d) Energy levels of ADT, TP, ADPD, 4F1NTP, and 4F2NTP obtained from cyclic voltammetry methods.

exhibit very similar absorption band with the maxima peaks at 643, 637, 635, and 646 nm, respectively, corresponding to their $S_0 \rightarrow S_1$ transitions. The absorption maximum of ADT is observed at a much lower wavelength of 555 nm, consistent with its larger HOMO–LUMO gap. The $S_0 \rightarrow S_2$ transitions are observed at 422, 440, 437, 438, and 439 nm for ADT, TP, ADPD, 4F1NTP, and 4F2NTP, respectively.

The fluorescence emission spectra of ADT, TP, ADPD, 4F1NTP, and 4F2NTP in toluene solutions were measured with an optical density less than 0.1 at the excitation wavelength (Figure 2b). The fluorescence peaks of ADT, TP, ADPD, 4F1NTP, and 4F2NTP molecules are located at 573, 664, 658, 657, and 670 nm, respectively. The energy of singlet excitons, $E(S_1)$, can be obtained from the energy-averaged maxima of the absorption and emission spectra of the heteroarenes. The $E(S_1)$ of ADT, TP, ADPD, 4F1NTP, and 4F2NTP molecules are determined to be 2.20, 1.90, 1.91, 1.92, and 1.88 eV, respectively. Table 1 summarizes the detailed spectroscopic data.

The phosphorescence spectra of heteroarenes are generally weak and have rarely been studied before. Herein, we successfully obtained the phosphorescence spectra of the five compounds in deoxygenated 2-methyltetrahydrofuran solutions at 77 K using liquid nitrogen as refrigerant. Figure 2c shows the phosphorescence spectra of the five compounds. For TP, the phosphorescence peak is observed at 1580 nm, in good

agreement with that reported by Zirzmeier¹⁵. The phosphorescence peaks of ADT, ADPD, 4F1NTP, and 4F2NTP occur at 1525, 1555, 1558, and 1602 nm, respectively, the triplet exciton energy $E(T_1)$ can be estimated from the deoxygenated phosphorescence peak positions, which give 0.81, 0.78, 0.80, 0.80, and 0.77 eV for the ADT, TP, ADPD, 4F1NTP, and 4F2NTP, respectively. With the above spectroscopic data, we can then obtain the ΔE_{SF} , using $\Delta E_{SF} = 2E(T_1) - E(S_1)$, which is -0.58 , -0.34 , -0.31 , -0.32 , and -0.34 eV for the ADT, TP, ADPD, 4F1NTP, and 4F2NTP, respectively. The ΔE_{SF} value for TP obtained from this work is consistent with that reported in literature,²³ confirming our measurements are reliable.

For SF process to efficiently take place, the ΔE_{SF} needs to be negative.^{44–46} The measured ΔE_{SF} indicates that all of the five molecules meet the basic energy conditions for SF. Among them, the ADT with electron-donating thiophene units shows the strongest exothermic effect, whereas ADPD and 4F1NTP with electron-drawing pyridine and tetrafluorobenzene groups, respectively, release the least energies during SF processes. Among the five molecules, TP and 4F2NTP have nearly the same moderate driving forces. The tunability of ΔE_{SF} through chemical modification enables dissection of the relationship between ΔE_{SF} and triplet excitation efficiency.

To probe the effects of the ΔE_{SF} on the magnitude of SF, femtosecond transient absorption (fsTA) spectroscopy was used to characterize the photogeneration and dynamic behaviors of the excited states in the concentrated solutions (0.02 M) of ADT, TP, ADPD, 4F1NTP, and 4F2NTP. Figure 3a shows three types of bands in the spectra of ADT, including the positive absorption band from 450 to 550 nm, the negative absorption band centered at about 570 and 610 nm, and the broad positive absorption band from 630 to 780 nm. When the delay time was prolonged, the intensity of the peak around 500 nm decreased, attributed to the $S_1 \rightarrow S_n$ transition, while the intensity of peak around 728 nm increased. Simultaneously, a particularly noticeable effect was shown in ADT, which is the red shift of the ground state bleaching (GSB), from 604 to 608 nm,¹⁵ accompanied by an intensification of the transient bleaching, indicative of SF. We have previously reported that TP and ADPD show efficient SF in solid state,²⁸ while the fsTA spectra obtained herein indicated that they also exhibit SF phenomena in solution. TP and ADPD in solutions exhibited short-lived positive absorption peaks at 464 and 514 nm, and 466 and 525 nm, respectively, which are assigned to the $S_1 \rightarrow S_n$ transition. Meanwhile, negative absorption peaks at 650 and 642 nm for TP and ADPD increased (Figure 3b,c), and resembled those of the lowest energy transition of the ground-state absorption spectra, which is attributed to the GSB. After hundreds of picoseconds, the initial positive absorption peaks at 466 and 512 nm are for TP and 466 and 525 nm are for ADPD

Table 1. Detail Data of $E(S_1)$, $E(T_1)$, and ΔE_{SF} of ADT, TP, ADPD, 4F1NTP, and 4F2NTP in Concentrated Toluene Solutions

sample	λ_{abs}/nm	λ_{fl}/nm	$E(S_1)/eV^{a}$	λ_{ph}/nm	$E(T_1)/eV^b$	$\Delta E_{SF}/eV^c$	$\phi_t/\%^d$
ADT	555, 422	574	2.20	1525	0.81	-0.58	117%
TP	643, 440	664	1.90	1580	0.78	-0.34	124%
ADPD	637, 437	659	1.91	1555	0.80	-0.31	140%
4F1NTP	635, 438	659	1.92	1558	0.80	-0.32	132%
4F2NTP	646, 439	671	1.88	1602	0.77	-0.34	136%

^a $E(S_1)$ is calculated from the mean peaks of UV–vis absorption and fluorescence spectra of sample in solutions, that is, $E(S_1) = 1240/\lambda$. ^b $E(T_1)$ is due to phosphorescence spectra at 77 K with the formula $E(T_1) = 1240/\lambda$. ^c ΔE_{SF} is defined as thermodynamic driving force for singlet exciton fission. $\Delta E_{SF} = 2E(T_1) - E(S_1)$. ^d ϕ_t is the triplet exciton yields due to singlet exciton fission.

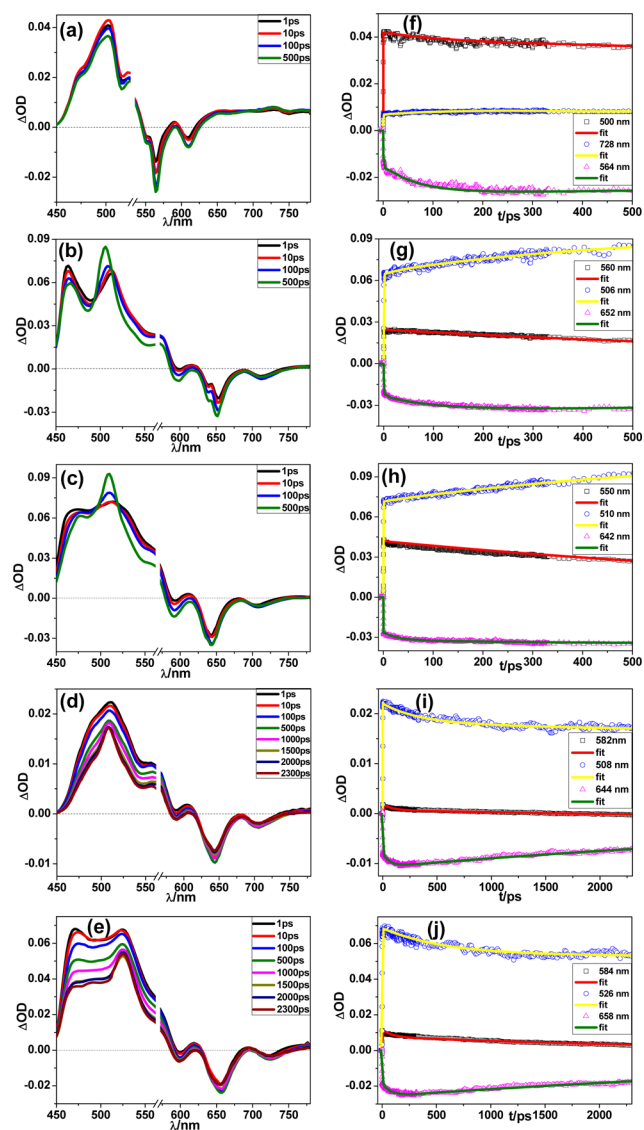


Figure 3. Ultrafast transient absorption spectra of (a) ADT excited at 530 nm, (b) TP, (c) ADPD, (d) 4F1NTP, and (e) 4F2NTP excited at 567 nm in 0.02 M toluene solutions. For these five compounds, the initial excited population is composed of singlets. Substantial triplet growth occurs from about hundreds of picoseconds as indicated by the absorptions at 728, 506, 510, 506, and 526 nm for ADT, TP, ADPD, 4F1NTP, and 4F2NTP, respectively, and are accompanied by accelerated singlet decay at 500, 464, 466, 466, and 472 nm for ADT, TP, ADPD, 4F1NTP, and 4F2NTP, respectively. Representative dynamic curves were characterized and fitted for ADT (f), TP (g), ADPD (h), 4F1NTP (i), and 4F2NTP (j).

decay, while the absorption peaks at 505 nm for TP and 510 nm for ADPD rose significantly due to $T_1 \rightarrow T_n$ transition. Minor rising absorption peaks at 470 and 476 nm were due to the secondary vibration peaks of $T_1 \rightarrow T_n$ transitions. The arising absorption peaks agreed with the previous reports for TP triplet states in solutions.^{13,15,16} Stern et al. have reported the significant stabilization of triplet pair state, i.e., excimer, of tetracene due to endothermic effect.⁴⁶ In contrast, the SF of our molecules shows obvious exothermal effect, in which the released heat provided energy necessary to disassemble the excimer into two free triplet excitons, so that the excimer splits into two triplets in a much faster fashion than that under endothermic condition. This fact is evident in the transient

absorption spectra, in which no spectral feature corresponding to the excimer can be observed, indicating a much shorter excimer lifetime.

For fluorine-substituted heteroarenes of 4F1NTP and 4F2NTP, there are two parts in their spectra at 567 nm excitation, including strong positive part from 450 to 580 nm and two negative peaks, 638 and 708 nm for 4F1NTP and 658 and 724 nm for 4F2NTP. Peaks at 466 and 472 nm were noted in terms of the singlet excited state characteristics. As time prolonged, the relative intensity of the 506 nm peak for 4F1NTP and the 526 nm peak for 4F2NTP increased notably, as shown in Figure 3d,e, attributed to the formation of triplet excitons. Minor rising absorption peaks at 472 nm for 4F1NTP and 488 nm for 4F2NTP were due to the secondary vibration peaks of $T_1 \rightarrow T_n$ transitions. Moreover, the negative peaks at 638 and 658 nm correspond to GSB for 4F1NTP and 4F2NTP, respectively. The other negative peaks at 708 and 728 nm are assigned to stimulated emission for 4F1NTP and 4F2NTP, respectively.¹⁵

The dynamic traces of ADT, TP, ADPD, 4F1NTP, and 4F2NTP and their corresponding fitted curves are shown in Figure 3f–j. As shown in the dynamic curves of ADT, the singlet exciton photoinduced absorption (PIA) at 500 nm decays with the time, accompanied by the increase of triplet exciton PIA at 728 nm. Similar phenomenon is also present in TP and ADPD. In the solutions of TP and ADPD, the peaks of singlet exciton PIA at 464 and 466 nm decay rapidly, along with the increase of the corresponding triplet exciton PIA at 506 and 510 nm. For the fluorinated heteroarenes, the intensity of singlet exciton PIA at 466 and 472 nm for 4F1NTP and 4F2NTP notably decreased, and that of triplet exciton PIA at 506 and 526 nm increased as time proceeded. The fast decay of singlet excitons to long-lived triplet excitons with high yields is a direct evidence of efficient SF taking place in the solutions.

Because the triplet excitons of these heteroarenes have lifetimes in the range of microseconds, we have also investigated the nanosecond transient absorption spectra of the *N*-heteropentacene to unveil their triplet exciton properties. Figure 4a–e showed the transient absorption spectra of the five compounds in solutions with same concentration of 10^{-4} M. For the ADT, TP, ADPD, 4F1NTP, and 4F2NTP, the singlet excited states are the short-lived, negative peaks at 620, 645, 640, 638, and 658 nm, while the triplet excited states are the intense, long-lived, positive excited-state absorption peaks at 728, 506, 510, 506, and 526 nm, respectively. Also, there are secondary vibration peaks measured at 470, 475, 472, and 488 nm for TP, ADPD, 4F1NTP, and 4F2NTP, respectively, consistent with the above fsTA spectra and that reported before for TP.²³ From Figure 4a–e, we can see that the decay times from singlet excitons to their corresponding triplet excitons are relatively slow in dilute solutions and lasted for a dozen nanoseconds, suggesting that the main exciton decay channel is intersystem-crossing. The resulting triplet excitons deactivate with a long lifetime to the ground states, in several microseconds.¹⁵

Nanosecond transient absorption spectrum of a 0.02 M TP solution was shown in Figure 4g for comparison. The strong and long-lifetime excited-state absorption located at 506 nm is attributed to the triplet exciton PIA. The lifetimes of triplet exciton PIA and GSB are almost identical, indicating that these two processes are strongly correlated with each other. The lifetime of the triplet exciton is about 33.6 μ s in concentrated solution, much longer than that of the dilute solution (1.67 μ s),

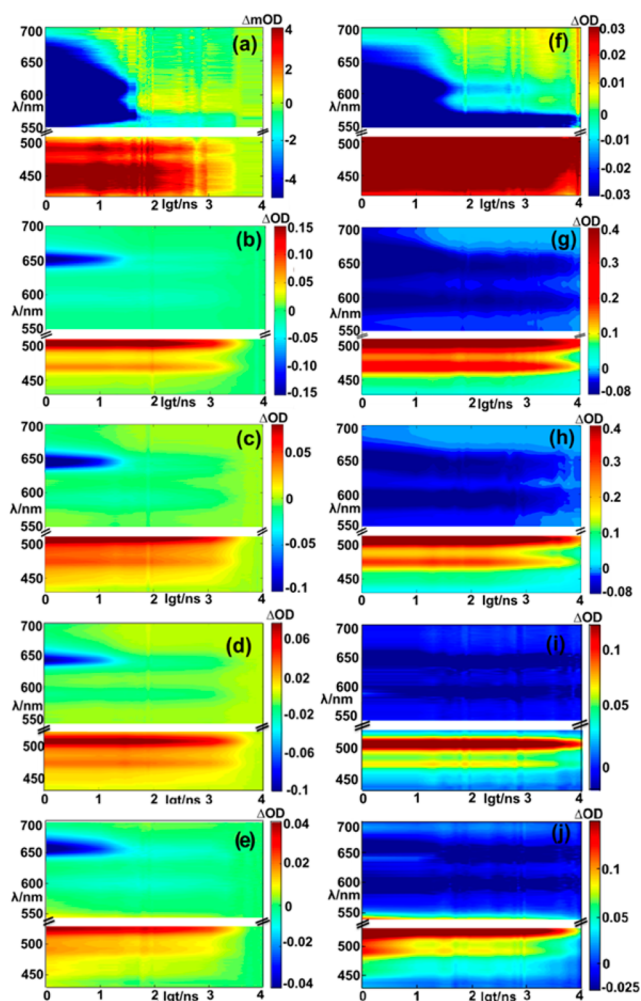


Figure 4. Nanosecond transient absorption spectra of ADT solution of (a) 10^{-4} M, (f) 0.02 M; TP solution of (b) 10^{-4} M, (g) 0.02 M; ADPD solution of (c) 10^{-4} M, (h) 0.02 M; 4F1NTP solutions of (d) 10^{-4} M, (i) 0.02 M 4F1NTP; and 4F2NTP solutions of (e) 10^{-4} M, (j) 0.02 M with triplet features at 728, 506, 510, 506, 516 nm, respectively.

which is clearly different from that of the singlet exciton (15 ns). The strongly correlated triplet excitons PIA and GSB lifetime, along with the long lifetime of triplet exciton confirmed that the main exciton decay route in the concentrated solution is SF, which is clearly different from that in the diluted solution. Similarly, the comparison between the nanosecond transient absorption spectra of ADT, ADPD, 4F1NTP, and 4F2NTP in solution of different concentrations indicated that SF process took place in their concentrated solutions.

We then evaluated the SF-induced triplet yields of the five compounds by monitoring the increment of the GSB band, which is accompanied by the corresponding positive absorption changes resulting from the generation of two triplet states.^{15,28} The detailed process is presented in the [Supporting Information](#). The calculated triplet exciton yields are 117% for ADT, 124% for TP, 140% for ADPD, 132% for 4F1NTP, and 136% for 4F2NTP. It is noted that the triplet yield for TP is somehow lower than that reported by Friend,²³ which is reasonable as the solution concentration in this study is much lower. Because the maximum solubility is about 0.02 M for 4F1NTP and 4F2NTP, this concentration was adopted for the

two molecules. Furthermore, we also studied the solutions of ADT, TP, and ADPD with higher concentration of 0.05 M, in which the triplet yields of ADT, TP, and ADPD increased to 161%, 172%, and 185% ([Figure S6](#)), confirming that higher concentration increases the triplet yield, and agrees well with that reported in literature.²³

It is noted that ADT has the highest driving force for SF, but its yield of triplet exciton is the lowest in either the 0.02 or the 0.05 M solutions. While ADPD and 4F1NTP have the lowest driving force for SF, the corresponding triplet exciton yields are almost the highest in contrast. The data also reveals that the relation between the driving force ΔE_{SF} and triplet yield is obviously not linear. It is noted that 4F2NTP is somehow an exception in this series. Although 4F2NTP has nearly the same driving force with TP, it exhibits higher triplet yield. The introduction of electron-drawing fluorine atoms endowed 4F2NTP with longer phosphorescence lifetime than that of TP ([Figure S5a](#) in [Supporting Information](#)), which may account for the higher triplet yield of the former. We thus infer the molecular structure is an important factor influencing the process of SF. How electron-drawing fluorine atoms influence SF process is worthy of further systematic study.

In most physical chemistry processes, it is generally expected that a higher driving force shall lead to a higher transition efficiency. However, the relationship between the magnitude of ΔE_{SF} and the degree of SF efficiency suggests an interesting result that a larger absolute value of ΔE_{SF} does not necessarily lead to a higher SF efficiency. Particularly, the ADT molecule has the largest ΔE_{SF} but gives the lowest SF efficiency. The results from this work indicate that excessive exoergicity can lower the SF efficiency in solutions. The most reasonable explanation to this somehow unexpected result is that the excessive exoergicity would cause a loss of efficiency by heat generation and enhance other relaxation channels that compete with SF, leading to a low triplet yield for SF. As shown in [Figure 1b](#), the competing channels may include fluorescence from the singlet state or excimer and nonradiative relaxation. Furthermore, we conducted experiments on dynamic behaviors of the excimers in the concentrated solutions. From the dynamic curves ([Figure S4](#) in [Supporting Information](#)), the decay of concentrated TP and ADPD was much faster (1.2 and 1.6 ns, respectively) than that of ADT, which showed a slow breaking up of the excimer of 2.7 ns to two triplet exciton-bearing free molecules.²¹ The slower formation of free triplet excitons enhanced other competing decay channels including excimer fluorescence and nonradiative relaxation, and as a result for ADT, relatively low triplet yield was obtained even with higher driving force. In addition, it is noted that $E(S_1)$ (2.20 eV) of ADT is close to the three times of $E(T_1)$ of 2.43 eV. Therefore, with extra energy from the common SF process, direct fission of ADT singlet into three triplets is possible,¹⁶ although unlikely since the probability for quick formation of trimer excited state in solution shall be extremely low. The above findings are important for understanding the SF in solution, which indicates the essential importance of the control over the thermodynamic driving force in the design of organic materials for high triplet yields based on SF mechanism.

We have also measured the phosphorescence lifetime of the five heteroacenes. [Figure S5a](#) illustrates the decay curves of ADT, TP, ADPD, 4F1NTP, and 4F2NTP in toluene solutions. The data fitting give lifetimes of 13.41, 12.93, 13.85, 15.51, and 15.80 μ s for ADT, TP, ADPD, 4F1NTP, and 4F2NTP,

respectively (Table S1). Such sufficiently long lifetimes of the triplet state would be key for potential applications.

One important requirement for efficient SF is a strong interaction between the singlet exciton with a nearby ground state molecule, which is unfortunately also an ideal scenario for photochemical reaction to occur. Therefore, acenes with high SF efficiency generally exhibit poor photostability, which become a big obstacle for their application. For example, the easy degradation of pentacene due to photooxidation and dimerization prevents it from being used in applications in the presence of light and air.^{47,48} Functionalization of acenes can be a good method to regulate the photostability⁴⁹ and photoelectric properties. We have demonstrated that the introduction of heterocycle units like thiophene and pyridine units and electron-drawing fluorinated atoms into the acene framework may dramatically increase their photostabilities.^{40,43}

Figure S5b shows the photostability of these heteroacenes in toluene solutions, which is obtained by monitoring the decay of the maxima absorbance wavelength under UV irradiation. The stability curve shows that the absorbance of TP decayed to half of the initial value after 1 week. In contrast, for ADT, ADPD, 4F1NTP, and 4F2NTP, their absorbance decay is less than 10% within a week. The photostability of the ADT, ADPD, 4F1NTP, and 4F2NTP are greatly improved compared with TP, which is mainly attributed to their lower HOMOs than those of TP. The much higher photostability of the *N*-heteroacenes make them more applicable in electro-optic applications.^{50,51}

3. CONCLUSIONS

To summarize, we have conducted the first systematic examination SF efficiency in solutions of heteroacenes with two different concentrations. This systematic research provides insights on how the thermodynamic driving force, ΔE_{SF} , affects the SF efficiency of organic molecules in solutions. More specifically, we have first addressed the energy levels of triplet excitons in solutions of heteroacenes through phosphorescence measurement at 77 K, and then obtained the values of ΔE_{SF} and SF efficiency in solutions of heteroacenes through fsTA. The results of our study indicate that SF can occur fast and effectively in the solutions of ADT, TP, ADPD, 4F1NTP, and 4F2NTP. Our results help to understand how the molecular structure influences the process of SF. One important finding is that a slightly negative ΔE_{SF} is beneficial for SF, but excessive exothermicity would cause a loss of efficiency by promoting other competitive channels and increasing nonradiative decay. This is shown in ADT, which gives the lowest SF efficiency though the absolute value of ΔE_{SF} , and is the largest among the test molecules. In contrast, the ADPD and 4F1NTP with the smallest absolute value of ΔE_{SF} exhibit the highest SF efficiency. This result implies that ADT is suboptimal due to the excess energy wasted as heat. Unveiling the relationship between the magnitude of SF and the value of ΔE_{SF} is of great importance for designing novel organic materials with high triplet exciton yields for various applications. Besides the high efficiency of SF, we have demonstrated that the introduction of heterocycle units like thiophene, pyridine, pyrazine, and electron-drawing fluorobenzene units into the acene framework may dramatically increase their photostability. These findings provide basic guidelines for designing novel organic materials with both high SF efficiency and good photostability.

■ ASSOCIATED CONTENT

Supporting Information

The Supporting Information is available free of charge on the ACS Publications website at DOI: 10.1021/jacs.6b03829.

Details of experimental procedures, UV–visible spectra of films, cyclic voltammogram, dynamic curves of fluorescence spectra, femtosecond and nanosecond transient absorption spectroscopic properties and the determination of SF yields (PDF)

■ AUTHOR INFORMATION

Corresponding Authors

*hongbing.fu@iccas.ac.cn

*haoli.zhang@lzu.edu.cn

Notes

The authors declare no competing financial interest.

■ ACKNOWLEDGMENTS

This work is supported by National Basic Research Program of China (973 Program) No. 2012CB933102, National Natural Science Foundation of China (NSFC. 51525303, 21233001, 21190034, 21573251), the Fundamental Research Funds for the Central Universities (lzujbky-2015-18) and 111 Project.

■ REFERENCES

- (1) Smith, M. B.; Michl, J. *Chem. Rev.* **2010**, *110*, 6891–6936.
- (2) Shockley, W.; Queisser, H. J. *J. Appl. Phys.* **1961**, *32*, 510–519.
- (3) Zhu, X. *Acc. Chem. Res.* **2013**, *46*, 1239–1241.
- (4) Yang, L.; Tabachnyk, M.; Bayliss, S. L.; Bohm, M. L.; Broch, K.; Greenham, N. C.; Friend, R. H.; Ehrler, B. *Nano Lett.* **2015**, *15*, 354–358.
- (5) Congreve, D. N.; Lee, J.; Thompson, N. J.; Hontz, E.; Yost, S. R.; Reuswig, P. D.; Bahlke, M. E.; Reineke, S.; Van Voorhis, T.; Baldo, M. A. *Science* **2013**, *340*, 334–337.
- (6) Lee, J.; Jadhav, P.; Reuswig, P. D.; Yost, S. R.; Thompson, N. J.; Congreve, D. N.; Hontz, E.; Van Voorhis, T.; Baldo, M. A. *Acc. Chem. Res.* **2013**, *46*, 1300–1311.
- (7) Busby, E.; Xia, J.; Wu, Q.; Low, J. Z.; Song, R.; Miller, J. R.; Zhu, X. Y.; Campos, L. M.; Sfeir, M. Y. *Nat. Mater.* **2015**, *14*, 426–433.
- (8) Schrauben, J. N.; Ryerson, J. L.; Michl, J.; Johnson, J. C. *J. Am. Chem. Soc.* **2014**, *136*, 7363–7373.
- (9) Musser, A. J.; Al-Hashimi, M.; Maiuri, M.; Brida, D.; Heeney, M.; Cerullo, G.; Friend, R. H.; Clark, J. *J. Am. Chem. Soc.* **2013**, *135*, 12747–12754.
- (10) Eaton, S. W.; Shoer, L. E.; Karlen, S. D.; Dyar, S. M.; Margulies, E. A.; Veldkamp, B. S.; Ramanan, C.; Hartzler, D. A.; Savikhin, S.; Marks, T. J.; Wasielewski, M. R. *J. Am. Chem. Soc.* **2013**, *135*, 14701–14712.
- (11) Kasai, Y.; Tamai, Y.; Ohkita, H.; Bente, H.; Ito, S. *J. Am. Chem. Soc.* **2015**, *137*, 15980–15983.
- (12) Varnavski, O.; Abeyasinghe, N.; Arago, J.; Serrano-Perez, J. J.; Orti, E.; Lopez Navarrete, J. T.; Takimiya, K.; Casanova, D.; Casado, J.; Goodson, T., 3rd. *J. Phys. Chem. Lett.* **2015**, *6*, 1375–1384.
- (13) Pensack, R. D.; Tilley, A. J.; Parkin, S. R.; Lee, T. S.; Payne, M. M.; Gao, D.; Jahnke, A. A.; Oblinsky, D. G.; Li, P. F.; Anthony, J. E.; Seferos, D. S.; Scholes, G. D. *J. Am. Chem. Soc.* **2015**, *137*, 6790–6803.
- (14) Sanders, S. N.; Kumarasamy, E.; Pun, A. B.; Trinh, M. T.; Choi, B.; Xia, J.; Taffet, E. J.; Low, J. Z.; Miller, J. R.; Roy, X.; Zhu, X. Y.; Steigerwald, M. L.; Sfeir, M. Y.; Campos, L. M. *J. Am. Chem. Soc.* **2015**, *137*, 8965–8972.
- (15) Zirzmeier, J.; Lehnerr, D.; Coto, P. B.; Chernick, E. T.; Casillas, R.; Basel, B. S.; Thoss, M.; Tykewinski, R. R.; Guldi, D. M. *Proc. Natl. Acad. Sci. U. S. A.* **2015**, *112*, 5325–5330.
- (16) Busby, E.; Berkelbach, T. C.; Kumar, B.; Chernikov, A.; Zhong, Y.; Hlaing, H.; Zhu, X. Y.; Heinz, T. F.; Hybertsen, M. S.; Sfeir, M. Y.

Reichman, D. R.; Nuckolls, C.; Yaffe, O. *J. Am. Chem. Soc.* **2014**, *136*, 10654–10660.

(17) Thompson, N. J.; Wilson, M. W.; Congreve, D. N.; Brown, P. R.; Scherer, J. M.; Bischof, T. S.; Wu, M.; Geva, N.; Welborn, M.; Voorhis, T. V.; Bulovic, V.; Bawendi, M. G.; Baldo, M. A. *Nat. Mater.* **2014**, *13*, 1039–1043.

(18) Lukman, S.; Musser, A. J.; Chen, K.; Athanasopoulos, S.; Yong, C. K.; Zeng, Z. B.; Ye, Q.; Chi, C. Y.; Hodgkiss, J. M.; Wu, J. S.; Friend, R. H.; Greenham, N. C. *Adv. Funct. Mater.* **2015**, *25*, 5452–5461.

(19) Arias, D. H.; Ryerson, J. L.; Cook, J. D.; Damrauer, N. H.; Johnson, J. C. *Chem. Sci.* **2016**, *7*, 1185–1191.

(20) Korovina, N. V.; Das, S.; Nett, Z.; Feng, X.; Joy, J.; Haiges, R.; Krylov, A. I.; Bradforth, S. E.; Thompson, M. E. *J. Am. Chem. Soc.* **2016**, *138*, 617–627.

(21) Stern, H. L.; Musser, A. J.; Gelin, S.; Parkinson, P.; Herz, L. M.; Bruzek, M. J.; Anthony, J.; Friend, R. H.; Walker, B. J. *Proc. Natl. Acad. Sci. U. S. A.* **2015**, *112*, 7656–7661.

(22) Wan, Y.; Guo, Z.; Zhu, T.; Yan, S.; Johnson, J.; Huang, L. *Nat. Chem.* **2015**, *7*, 785–792.

(23) Walker, B. J.; Musser, A. J.; Beljonne, D.; Friend, R. H. *Nat. Chem.* **2013**, *5*, 1019–1024.

(24) Sanders, S. N.; Kumarasamy, E.; Pun, A. B.; Steigerwald, M. L.; Sfeir, M. Y.; Campos, L. M. *Angew. Chem., Int. Ed.* **2016**, *55*, 3373–3377.

(25) Monahan, N.; Zhu, X. Y. *Annu. Rev. Phys. Chem.* **2015**, *66*, 601–618.

(26) Hartnett, P. E.; Margulies, E. A.; Mauck, C. M.; Miller, S. A.; Wu, Y.; Wu, Y. L.; Marks, T. J.; Wasielewski, M. R. *J. Phys. Chem. B* **2016**, *120*, 1357–1366.

(27) Ryno, S. M.; Risko, C.; Bredas, J. L. *J. Am. Chem. Soc.* **2014**, *136*, 6421–6427.

(28) Wu, Y.; Liu, K.; Liu, H.; Zhang, Y.; Zhang, H.; Yao, J.; Fu, H. *J. Phys. Chem. Lett.* **2014**, *5*, 3451–3455.

(29) Zimmerman, P. M.; Musgrave, C. B.; Head-Gordon, M. *Acc. Chem. Res.* **2013**, *46*, 1339–1347.

(30) Johnson, J. C.; Nozik, A. J.; Michl, J. *Acc. Chem. Res.* **2013**, *46*, 1290–1299.

(31) Tomkiewicz, Y. *J. Chem. Phys.* **1971**, *54*, 4504–4507.

(32) Chan, W. L.; Ligges, M.; Zhu, X. Y. *Nat. Chem.* **2012**, *4*, 840–845.

(33) Zimmerman, P. M.; Zhang, Z.; Musgrave, C. B. *Nat. Chem.* **2010**, *2*, 648–652.

(34) Chan, W. L.; Ligges, M.; Jailaubekov, A.; Kaake, L.; Miaja-Avila, L.; Zhu, X. Y. *Science* **2011**, *334*, 1541–1545.

(35) Aragón, J.; Troisi, A. *Phys. Rev. Lett.* **2015**, *114*, 026402.

(36) Roberts, S. T.; McAnally, R. E.; Mastron, J. N.; Webber, D. H.; Whited, M. T.; Brutchey, R. L.; Thompson, M. E.; Bradforth, S. E. *J. Am. Chem. Soc.* **2012**, *134*, 6388–6400.

(37) Liu, Y.; Zhang, C.; Wang, R.; Zhang, B.; Tan, Z.; Wang, X.; Xiao, M. *Angew. Chem., Int. Ed.* **2015**, *54*, 6222–6226.

(38) Zhao, M.; Liu, K.; Zhang, Y.-D.; Wang, Q.; Li, Z.-G.; Song, Y.-L.; Zhang, H.-L. *Mater. Horiz.* **2015**, *2*, 619–624.

(39) Chen, Y.; Shen, L.; Li, X. *J. Phys. Chem. A* **2014**, *118*, 5700–5708.

(40) Liu, K.; Song, C.-L.; Zhou, Y.-C.; Zhou, X.-Y.; Pan, X.-J.; Cao, L.-Y.; Zhang, C.; Liu, Y.; Gong, X.; Zhang, H.-L. *J. Mater. Chem. C* **2015**, *3*, 4188–4196.

(41) Song, C. L.; Ma, C. B.; Yang, F.; Zeng, W. J.; Zhang, H. L.; Gong, X. *Org. Lett.* **2011**, *13*, 2880–2883.

(42) Liu, Y. Y.; Song, C. L.; Zeng, W. J.; Zhou, K. G.; Shi, Z. F.; Ma, C. B.; Yang, F.; Zhang, H. L.; Gong, X. *J. Am. Chem. Soc.* **2010**, *132*, 16349–16351.

(43) Wang, J.; Liu, K.; Liu, Y. Y.; Song, C. L.; Shi, Z. F.; Peng, J. B.; Zhang, H. L.; Cao, X. P. *Org. Lett.* **2009**, *11*, 2563–2566.

(44) Geacintov, N.; Pope, M.; Vogel, F. *Phys. Rev. Lett.* **1969**, *22*, 593–596.

(45) Burdett, J. J.; Muller, A. M.; Gosztola, D.; Bardeen, C. J. *J. Chem. Phys.* **2010**, *133*, 144506.

(46) Singh, S.; Jones, W. J.; Siebrand, W.; Stoicheff, B. P.; Schneider, W. G. *J. Chem. Phys.* **1965**, *42*, 330–342.

(47) Yamada, M.; Ikemoto, I.; Kuroda, H. *Bull. Chem. Soc. Jpn.* **1988**, *61*, 1057–1062.

(48) Liang, Z.; Zhao, W.; Wang, S.; Tang, Q.; Lam, S. C.; Miao, Q. *Org. Lett.* **2008**, *10*, 2007–2010.

(49) Kaur, I.; Stein, N. N.; Kopreski, R. P.; Miller, G. P. *J. Am. Chem. Soc.* **2009**, *131*, 3424–3425.

(50) Chaudhuri, D.; Sigmund, E.; Meyer, A.; Rock, L.; Klemm, P.; Lautenschlager, S.; Schmid, A.; Yost, S. R.; Van Voorhis, T.; Bange, S.; Hoger, S.; Lupton, J. M. *Angew. Chem., Int. Ed.* **2013**, *52*, 13449–13452.

(51) An, Z.; Zheng, C.; Tao, Y.; Chen, R.; Shi, H.; Chen, T.; Wang, Z.; Li, H.; Deng, R.; Liu, X.; Huang, W. *Nat. Mater.* **2015**, *14*, 685–690.